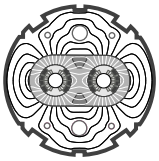

LHC Project Note 124

December 18, 1997

Thomas.Spickermann@cern.ch

Simulation of Point Beam Losses in LHC Superconducting Magnets

T. Spickermann, CERN-SL, GENEVA, Switzerland
K. Wittenburg, DESY, HAMBURG, Germany

Keywords: beam losses, quench protection

Abstract

The Monte Carlo shower codes GEANT3.21 [1] and FLUKA96 [2] have been used to simulate the impact of high energy protons ('point losses') on the aperture of superconducting magnets in the LHC arcs. These calculations allow to determine the efficiencies of various types of beam loss monitors for the LHC. The smallest number of lost protons that can be detected is compared to quench levels as computed in [3]. These studies show that point losses can be detected efficiently with monitors outside the vacuum vessel.

1 Introduction

The energy stored in the intense LHC beams is without precedence in any other accelerator. The effect of beam losses on superconducting magnets and other accelerator components is of major concern [4]. Fast and efficient beam loss monitors are required around the accelerator to help prevent magnet quenching and irradiation of sensitive components. The Monte Carlo shower codes GEANT3.21 and FLUKA96 have been used to determine the efficiency of different kinds of detectors. The quench levels, i.e. the numbers of lost protons that lead to a magnet quench have been computed in [3] for different loss durations. For 'medium range' losses, where the loss duration of a few milliseconds is comparable to the heat diffusion time constant of the coil, a quench occurs at about 10^6 lost protons per meter. A loss monitor system, to be able to provide an abort signal, should detect loss numbers significantly smaller than that in no more than 5 milliseconds. A loss detection system should also assist to diagnosis and tuning of the machine, which means that it should be sensitive to much smaller losses than what would be required to prevent quenches. Experience with DESY's HERA ring shows that beam loss monitors may also become very important in the detection of vacuum leaks.

2 Geometry

2.1 Half-cell in the Arc

The geometry used in the simulations contains the Short Straight Section (SSS) with a twin-aperture quadrupole (MQD/F), two octupoles (MOD/F) and two combined sextupole-dipole correctors (MSCBH/V), as well as surrounding dipoles plus correctors. The geometry description is based on [5], however, more recent drawings have been taken into account where available. The geometry has been largely simplified, so as to avoid an excessive number of boundaries and thus reduce computing time. Figure 1 shows a drawing of a detail of the geometry obtained with an interactive version of GEANT. The radiation shield, heat shield and vacuum vessel, though not shown in this drawing, are also taken into account. We define the direction along the beam which points from the quadrupole

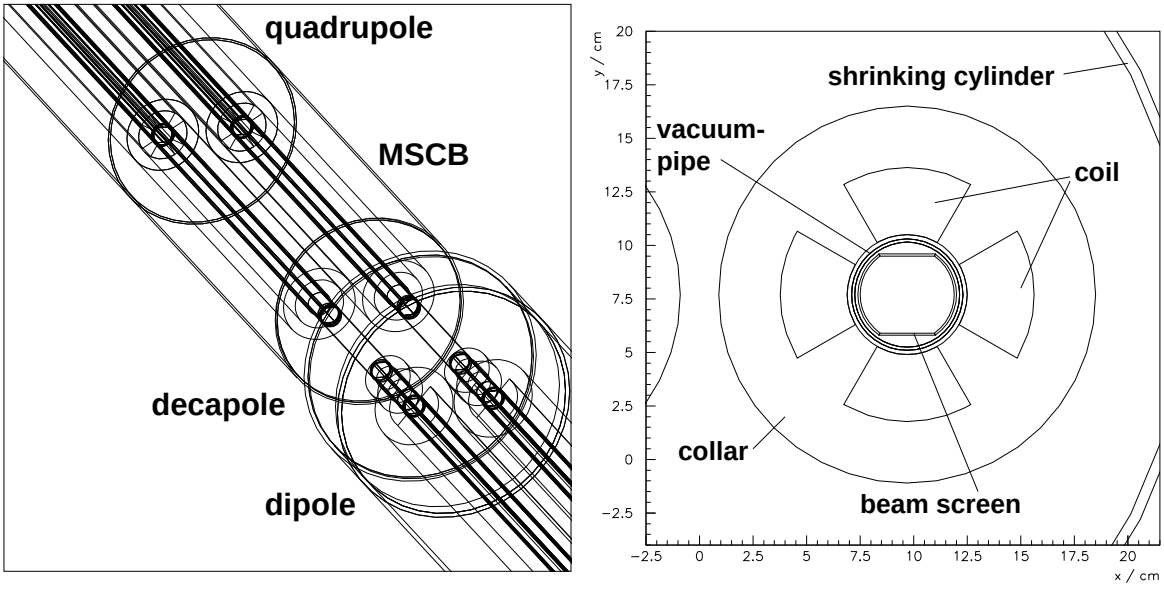

Figure 1: *left:* detail of the geometry, including quadrupole (right- and uppermost), MSCB, decapole and dipole
right: cross section through quadrupole, including beam screen, beam pipe, coil, collar, yoke and shrinking cylinder

to the MSCB as the positive s-direction. The centre of the quadrupole defines s=0.

2.2 Sensitive Volumes

Different types of loss monitors are simulated by adding sensitive volumes to the geometry of the half cell. A 5 cm thick cylinder filled with air is defined around the vacuum vessel and the energy deposit in this volume is calculated. This allows to estimate the sensitivity of ionization chambers at different positions outside the cryostat. Furthermore, the number of minimum ionising particles (MIPs) per lost proton that pass a certain area outside the cryostat can thus be determined.

To get an estimate on the sensitivity of the so-called 'micro-calorimeter' [6] a 1 cm thick copper disc is added just behind the quadrupole's cold-mass (i.e. behind the MSCB and the right end plate). The calculated energy deposit in the disc allows to determine the temperature increase in a copper block at such a position due to beam losses. For any calculations of rates behind the SSS (i.e. in the dipoles) this disc is of course removed from the geometry.

3 Procedure

We assume that point losses are most likely to occur in the middle of focusing quadrupoles, where both the beam size and the dispersion (for horizontally focusing quadrupoles) are maximum [5]. The aperture is limited by the beam screen [7] [8] [5], a device inserted into the beam pipe to intercept synchrotron radiation. The protons hit the beam screen in the middle of the quadrupole, at s=0, 'rightmost', i.e. at a maximum value of the horizontal transverse coordinate x (see figure 2). The protons point in the forward direction (towards the MSCB) in the horizontal plane. Impacts on the opposite side of the beam screen ('leftmost') are also simulated. The protons are incident on the beam screen with an angle of 0.25 mrad. Other angles of incidence have been used without much affecting the results.

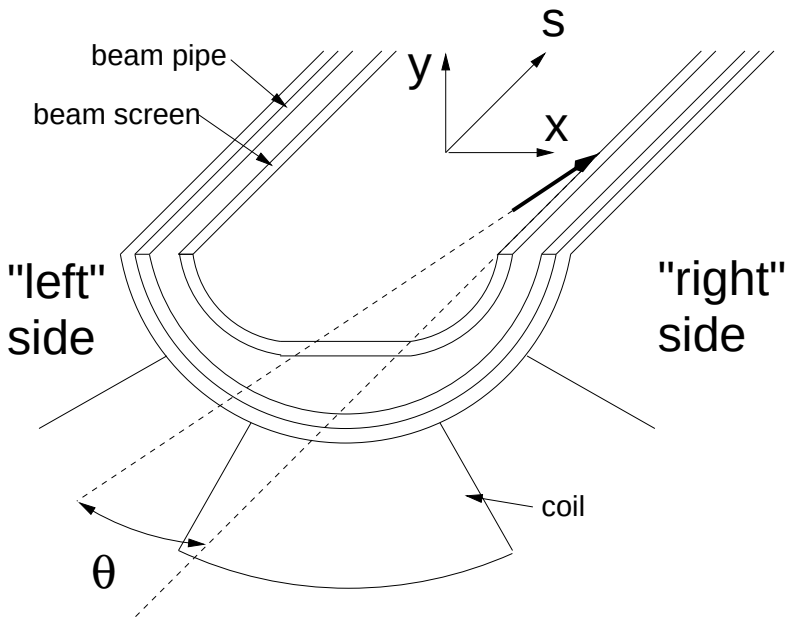

Figure 2: Protons are incident on the beam screen at s=0 (middle of quadrupole), x=maximum and θ=0.25 mrad.

Due to tolerances in the alignment of the beam screen losses are also to be expected in the extremities of the dipoles around the quadrupole [9] [10]. Such losses are also taken into account.
The incident proton interacts with a nucleus from the beam screen or other material, i.e. beam pipe or coil. The resulting hadronic shower is accompanied by an electro-magnetic

shower, due to the production of π^os and their subsequent decay into γs. GEANT3.21 uses by default the GHEISHA [11] package to describe hadronic interactions. The section PHYS in the GEANT3.21 manual [1] explains in detail the tracking steps and physics processes that occur in GEANT.

4 Energy deposit inside the cryostat

4.1 Energy deposit in magnet

As the shower develops through the magnet material, the produced particles lose energy in inelastic interactions with atoms along their track. The distribution of these energy losses along the shower is strongly correlated to the number of secondaries which is maximum at a certain distance of the incidence point. The distance depends on the energy of the incident proton as well as on the radiation length and the hadronic absorption length of the material. Figure 3 compares the mean energy deposit along s in coil and collar of the quadrupole for an incident proton energy of 7 TeV. Here the azimuthal angle Φ is measured in the x-y-plane from the centre of the beam pipe. By comparing the two scales in figure 3

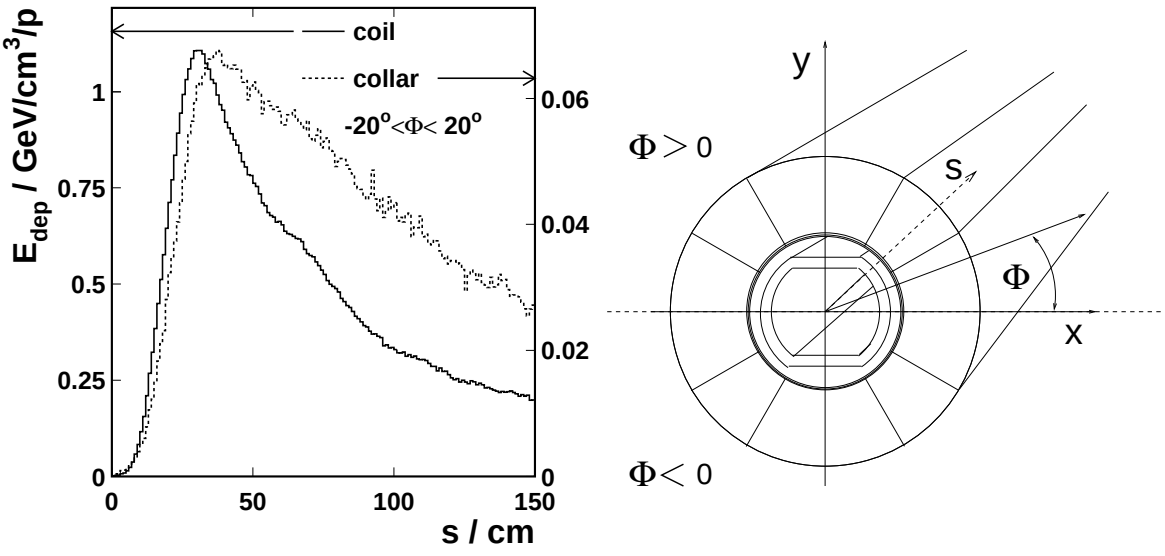

Figure 3: Energy deposit per lost proton along s in coil (left scale) and collar (right scale)

one notices that the energy deposit rapidly decreases from the inner to the outer part of the magnet. The energy lost from the shower particles is subsequently transferred into heat, via the production of phonons. A study of this 'heat load' was done in [3].

4.1.1 Importance of the magnetic field

The magnetic field [12] in the quadrupole as well as in the dipoles corresponding to a given beam energy has been taken into account in the simulation. Neglecting the field would

considerably reduce computing time, but also have a significant impact on the results of the simulation, as can be seen in figure 4 (note the different scales !). The presence of the

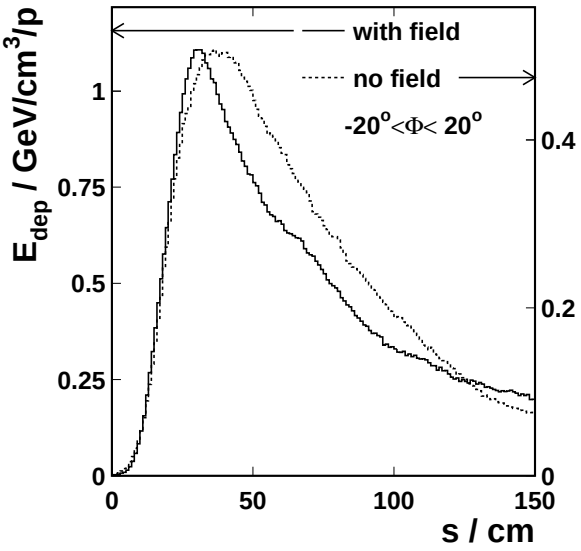

Figure 4: Energy deposit along s in coil with (left scale) and without magnetic field (right scale)

magnetic field about doubles the energy deposit. In addition the maximum is reached at a smaller value of s. Both effects stem from the fact that charged particles from the shower which enter the vacuum region of the beam pipe are drawn back into the material by the field.
Detection efficiencies are in the following all computed from the results obtained with magnetic field. Distributions obtained without magnetic field are nevertheless shown for completeness.

4.1.2 Comparison with FLUKA

The energy deposit in the coil (without magnetic field) has also been calculated with the program FLUKA [2]. Figure 5 compares the FLUKA result with that obtained with GEANT. The maximum of the distribution along s is higher in FLUKA and also slightly shifted to a higher value of s, however, the difference between the two distributions remains well within acceptable limits. A discussion of differences between GEANT and FLUKA would be beyond the scope of this report.

5 Loss detection

It is important to mention that the choice of detector types considered in the simulations is of course not complete. The aim of the present studies was not to decide on the most suitable detector type. Detectors not considered here, e.g. scintillators with photomultipliers should by no means be excluded on the basis of the results given here.

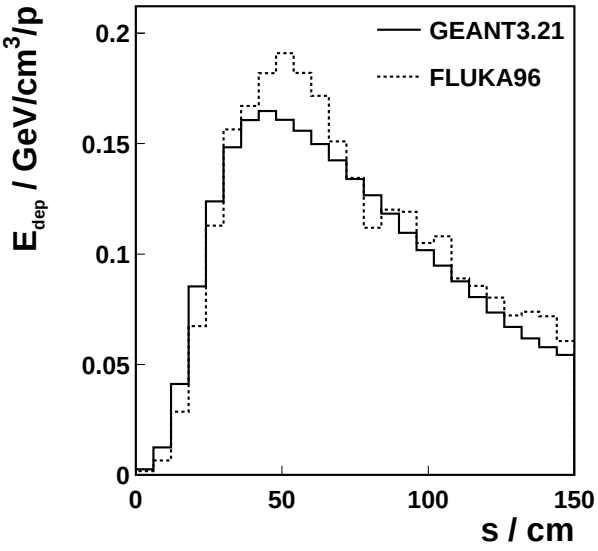

Figure 5: Energy deposit per lost proton along s in coil - Comparison between GEANT and FLUKA results

5.1 Detection inside the cryostat

5.1.1 Micro calorimeter

The temperature increase due to the energy loss of shower particles can be used for their detection. This was exploited in the proposal for the so-called micro calorimeter [6]. Copper blocks, connected to a thermoresistor, would be installed into the magnet's cold mass. In the 1.9 K environment of the cold mass one could measure temperature changes with a resolution of about 1 mK. The loss rate that would lead to such a temperature rise is determined with the simulation. In order to obtain results for different positions in one calculation, a copper disc of the same diameter as the magnet is defined at the end of the cold mass. Figure 6 shows the energy deposit in the copper disc behind the quadrupole cold mass.. The energy deposit per cm^3 of copper block along different x- and y-positions close to the beam pipe (see white lines in figure 6, right plot) is plotted in figure 7. A comparison of the GEANT results (without magnetic field) with FLUKA (see figure 8) gives a fairly good agreement between the two codes.
To compute the efficiency of the micro calorimeter we do not use the maximum in the distribution along y in figure 7, since that depends too much on the exact impact point of the proton. With the more realistic value of 0.05 Gev/cm^3 or $9{\cdot}10^{-13}$J/g per lost proton (7 TeV) and the specific heat of copper, c_p=$3{\cdot}10^{-5}$ J/g/K one obtains a temperature increase of $3{\cdot}10^{-5}$ mK/proton or 1 mK per 3300 lost protons. According to [6] the heating time constant τ of the micro calorimeter is about 0.5 s. With an exponential temperature rise

$$T = T_0 \cdot (1 - e^{t/\tau})$$

a temperature increase of 1 mK in 5 ms would require a total rise in temperature of 0.1 K. Thus, a loss of $3.3{\cdot}10^5$ protons could be detected in 5 ms. This value was obtained for

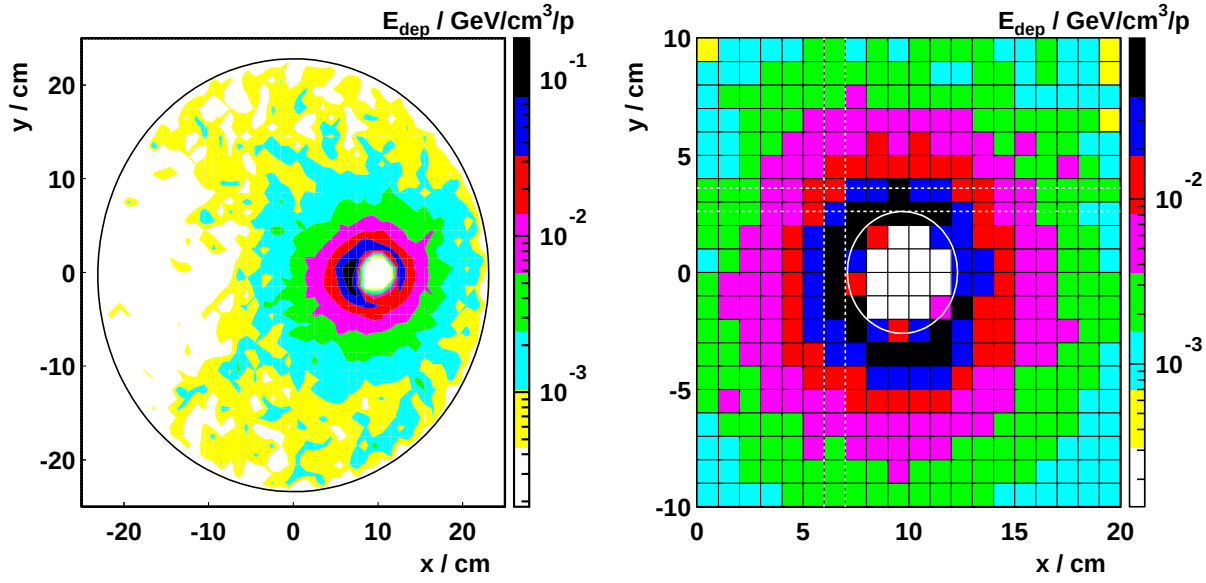

Figure 6: *left:* Energy deposit in a copper disc behind the quadrupole cold-mass
right: Close-up view around the right beam pipe

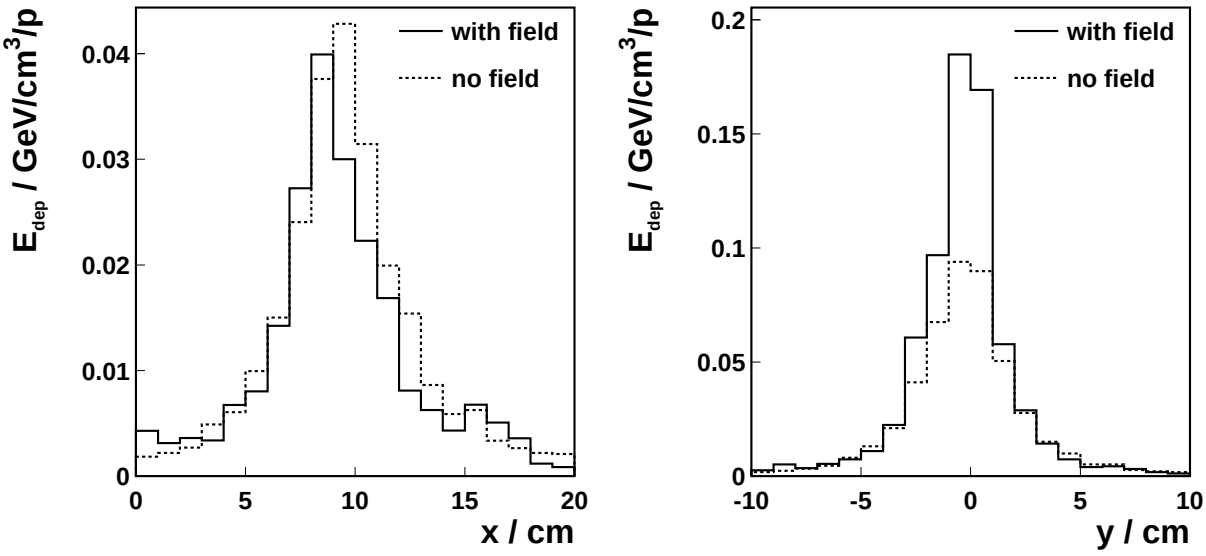

Figure 7: Energy deposit per cm^3 of copper along different x- and y-positions close to the beam pipe (see white lines in figure 6)

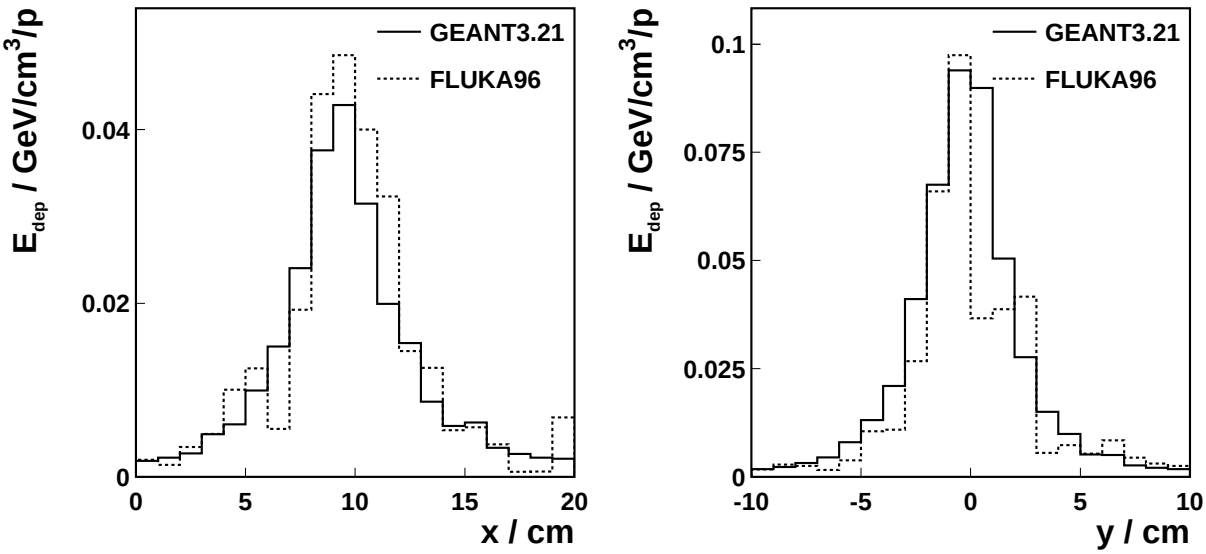

Figure 8: Energy deposit in a 1 cm^3 copper block positioned along different x- and y-positions - Comparison between GEANT and FLUKA

losses in the centre of the quadrupole. Figure 9 shows how the energy deposit and thus the efficiency depend on the longitudinal impact coordinate s of the losses. Similar simulations have been done for proton energies of 450 GeV (injection) and 1 TeV. The efficiency of the micro calorimeter is found to scale roughly with the proton energy.

5.2 Detection outside the vacuum vessel

Loss detectors outside the vacuum vessel would have the advantage of easier accessibility and positioning flexibility. Furthermore there are far less restrictions on the size of the detector, as opposed to the inside of the cryostat. Thus one can consider different types of detectors like ionization chambers, scintillation counters or semi-conductor devices. To determine whether the number of minimum ionising particles per area or the ionization energy loss (dE/dx) per unit volume around the vessel per lost proton will allow for efficient detection, we define as sensitive volume in the simulation a 5 cm thick cylinder around the vacuum vessel. The cylinder is filled with air at standard pressure.

5.2.1 PIN diodes

PIN diodes, which are at use as beam loss detectors in DESY's HERA ring [13] are sensitive to the passage of Minimum ionizing particles (MIPs). We use the following momentum cuts to define MIPs:

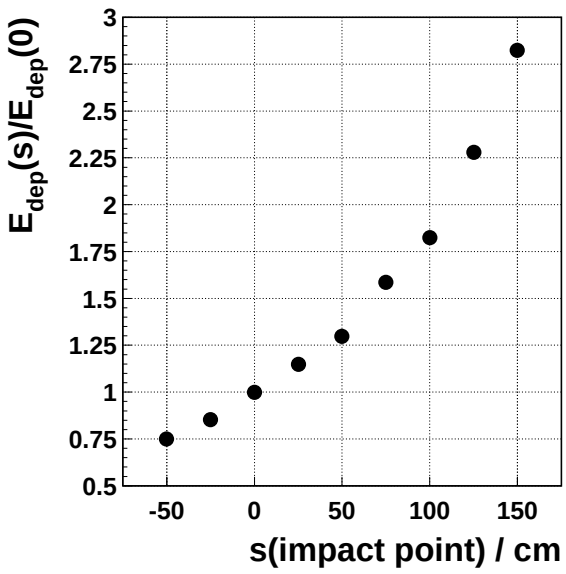

Figure 9: Dependence of the energy deposit in the micro calorimeter on the longitudinal impact coordinate of the proton

e^{+-}: p $\geq$ 0.3 MeV/c

μ^{+-},π^{+-}: p $\geq$ 15 MeV/c

p,$\bar{p}$,K^{+-}: p $\geq$ 140 MeV/c

The restriction to particles with momenta above these cuts serves mainly to limit computing time. In addition the GEANT code is less reliable for low-energetic particles. This restriction leads to an underestimate of the detection efficiency. Since particles with momenta below these cuts are much less likely to traverse the magnet material and reach the detector this error can be neglected.
Figure 10 shows the number of MIPs per cm^2 passing the vessel per lost proton (7 TeV). The angle Φ where the MIP distribution is maximum is about 10^o, since Φ is measured here from the centre of the vessel, which is lower than the centre of the magnet. The width of the longitudinal distribution in an angular region around the maximum is about 2 meter. This indicates that if the impact point of a proton varies along s by about 2 meter the detection efficiency would not drop significantly. It was so far assumed that the proton impacts on the right or outer edge of the beam screen. In a horizontally focusing quadrupole it may as well impact on the opposite (inner) side. Figure 11 compares the two cases. The maxima of the angular distribution in the two cases are at roughly the same angle, which comes from the fact that at $\Phi \approx 0$ (or $\Phi = 0$ if measured from the centre of the magnet) particles 'see' the least amount of material. The total number of MIPs in a region around the maximum is however smaller by a factor 2 in the case where the proton hits the beam screen on the left side. This is explained by the fact that a particle, to be detected in this region has first to traverse the beam screen. The angular distribution is also wider for impacts on the left side. This implies a higher 'cross talk', i.e. the probability that a

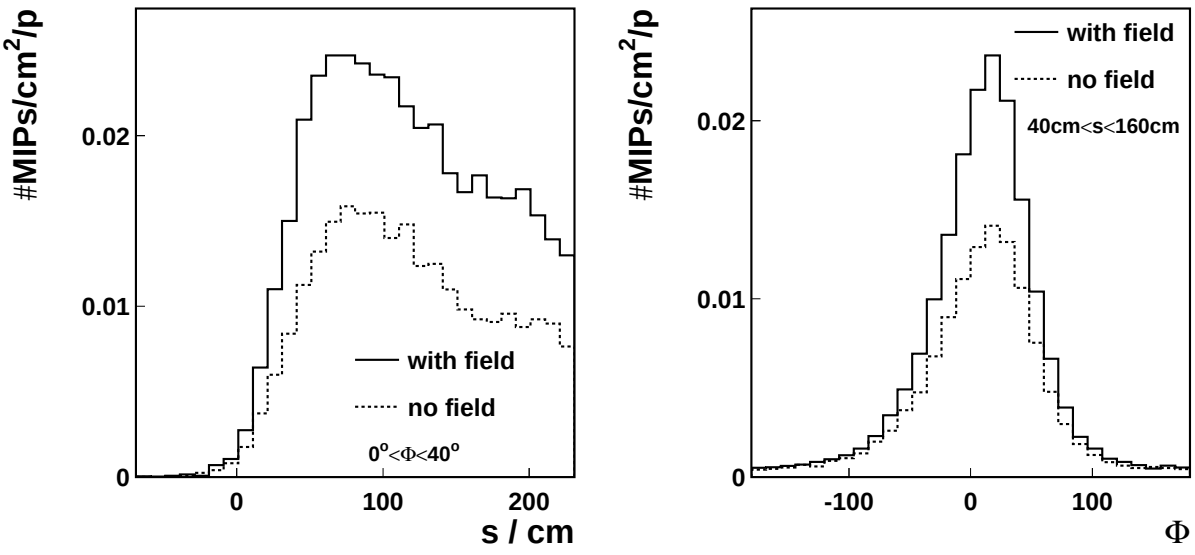

Figure 10: *left:* Longitudinal Distribution of MIPs outside the vacuum vessel *right:* Angular Distribution of MIPS. The angle Φ is measured here from the centre of the vessel

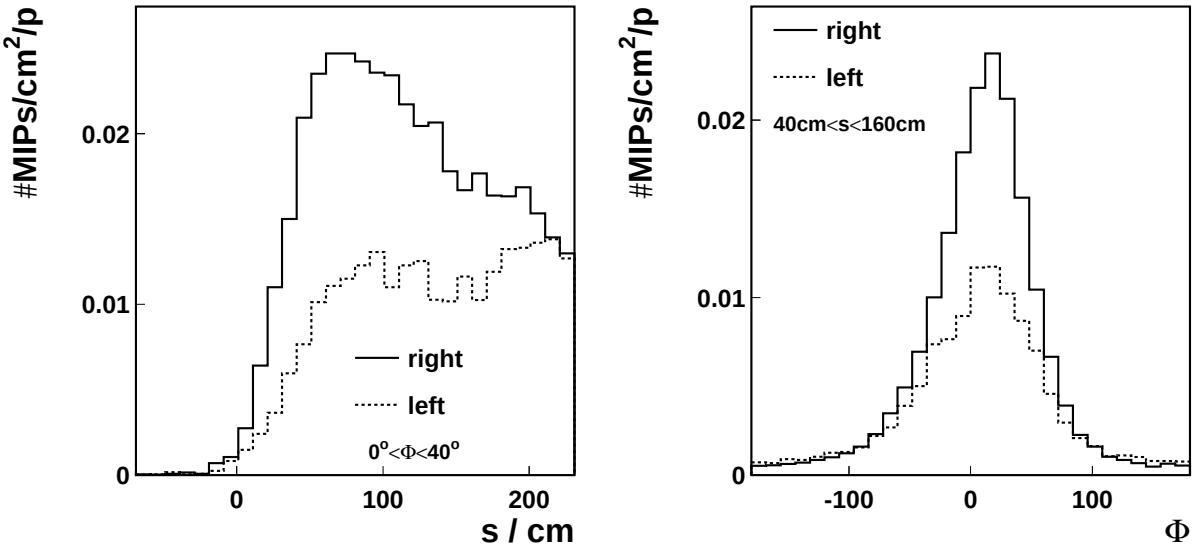

Figure 11: *left:* Longitudinal distribution of MIPs outside the vacuum vessel for impact of proton on the right side of the beam screen and on the left side (i.e. pointing towards centre of the magnet) *right:* Angular Distribution of MIPS for impact on right side and left side

particle which was lost in one beam pipe is wrongly attributed to a loss in the other pipe. The case where a proton is lost on the left side of the beam screen can thus be regarded as a 'worst case', concerning detection efficiency and cross talk. The efficiency of PIN diodes to detect MIPs has been measured to be 0.3 counts per MIP [14]. With 0.01 MIPs per cm^2 and lost proton a 1 cm^2 diode would therefore count $3{\cdot}10^{-3}$ MIPs per proton. Thus, a minimum of 330 lost protons can be detected at a beam energy of 7 TeV. The efficiency of 0.3 counts per MIP is only valid for a certain setting of threshold voltages. For this setting the noise rate of one diode is about 1 kHz. Thus, one count per 5 ms would yield a signal-to-noise ratio of 200. The noise can be further reduced by requiring a coincidence of the signal from two diodes on top of each other. The length of the coincidence signal is about 90 ns. A bunch spacing of 25 ns in the LHC [5] thus means that big loss rates can only be distinguished as such if they are distributed over significantly more than 3 bunches.

5.2.2 Ionization chambers

Ionization chambers are already in use as beam loss monitors at Fermilab's Tevatron [15]. The response to energy losses from charged particles has been measured to be 70 nC/rad, or $7{\cdot}10^{-6}$ C/Gy. The leakage current is about 10 pA, which would correspond to $5{\cdot}10^{-14}$ C/5ms.
Figure 12 shows the energy loss distribution in a 5 cm thick gas layer around the vacuum vessel. The energy deposition per lost proton can be taken from figure 12) to be $0.4{\cdot}10^{-11}$

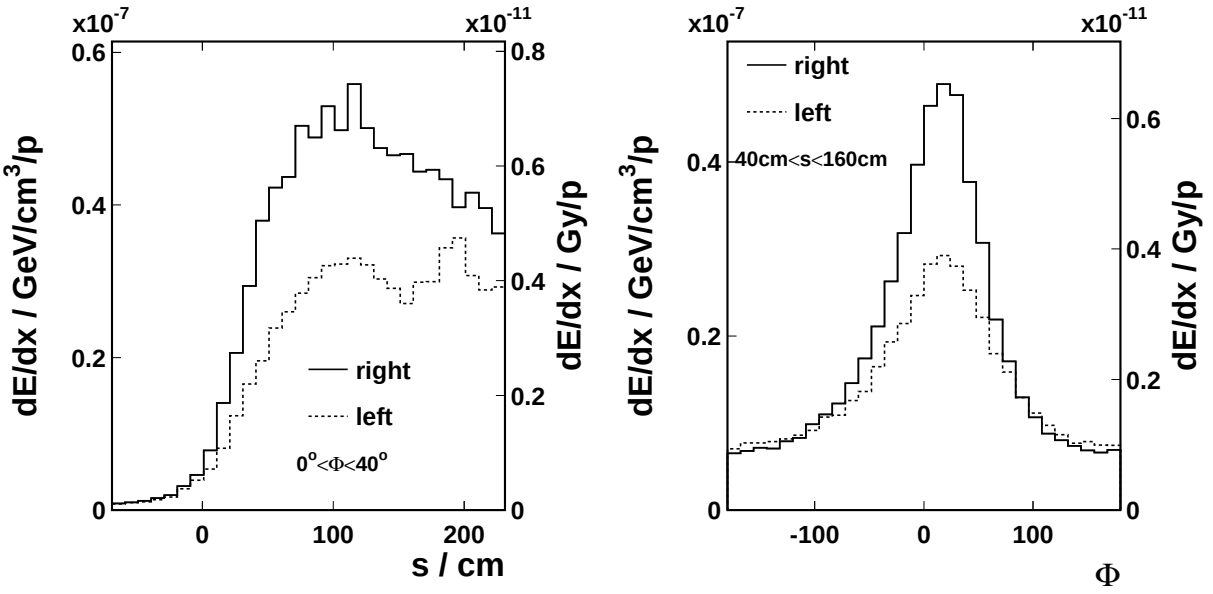

Figure 12: *left:* Longitudinal distribution of ionization energy loss in a 5 cm thick gas layer (air at standard pressure) for impact of proton on the right side of the beam screen and on the left side (i.e. pointing towards centre of the magnet)
right: Angular Distribution of ionization energy loss for impact on right side and left side

Gy/p (for impact on the left side). Thus, a loss of about 20,000 protons in 5 ms yields a signal-to-noise ratio of 10.

5.3 Comparison of detector sensitivity

The results given above have all been obtained for a proton energy of 7 TeV. The same simulations have been done for 450 GeV (injection energy) and for 1 TeV. Table 1 shows the minimum number of lost protons that can be detected with the methods discussed above for the different beam energies. Possible improvements of the sensitivity of the

beam energy	450 GeV	1 TeV	7 TeV
μcalorimeter	$3.7{\cdot}10^6$	$1.3{\cdot}10^6$	$3.3{\cdot}10^5$
ion. chamber	$1.2{\cdot}10^5$	$6{\cdot}10^4$	$2{\cdot}10^4$
PIN diodes	2,900	1,700	330

Table 1: Minimum number of lost protons that can be detected in 5 ms (proton incident on left side)

micro calorimeter are under study. For instance, replacing the copper block by a material with a smaller heat capacity could reduce the temperature rise time. Experiments with saphir (Al_2O_3) show that an improvement of the sensitivity by about a factor 10 may thus be achieved [16].
Both ionization chambers and PIN diodes would be able to detect losses significantly smaller than the quench levels computed in [3]. Other systems, e.g. scintillators with photo multipliers or -diodes could as well be considered.

6 Losses in dipoles

Large tolerances in the alignment of the beam screen may lead to losses in the entrance of the dipoles around the quadrupole in the arc [9] [10]. The geometry for dipoles, as it is used in the simulations described here, is very similar to that of quadrupoles, except for the larger length of the dipoles of about 14 m. Thus, the distributions of energy deposition and particle flow resemble those obtained for losses in quadrupoles. One exception stems from the difference in the form of the magnetic field inside the beam pipe. Charged particles from the shower which are emitted into the vacuum are either attracted back into the material or to the opposite side, depending on the sign of their charge. The latter is less likely to happen in quadrupoles, where the magnetic field seen by a particle traversing the beam pipe flips in the centre. For losses in dipoles one will thus expect a bigger 'cross talk', i.e. a higher probability, that a particle loss in one beam is detected on the opposite side of the vessel and assigned to the other beam (see figure 13).

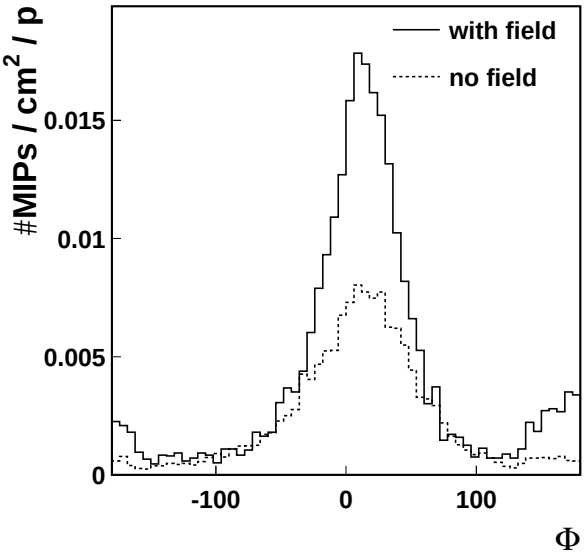

Figure 13: Angular distribution of MIPs for losses in a dipole. The 'cross talk', i.e. the signal on the side of the vessel opposite to the beam pipe where the loss occurred, stems from charged particles that are attracted to the opposite side by the magnetic dipole field.

7 Conclusion

Point losses of protons in the LHC arcs can be efficiently detected outside the vacuum vessel, where detectors would be accessible and flexible. Due to the effective shower length the point where protons are lost may vary by 1-2 meter without a significant decrease of the detection efficiency. The angular distribution of shower particles outside the vessel is determined by the geometry, allowing for an optimum angular positioning of the monitors.

8 Acknowledgements

We profited from most valuable support from Graham Stevenson, Harm Fesefeldt, Harry Renshall and Rüdiger Schmidt. Graham kindly provided the geometry for the FLUKA calculations. These were only possible thanks to the help from Jan Zazula, whom we shall gratefully remember. We would also like to express our gratitude to Laurentius Gatignon and Claude Bovet, who carefully proofread this note, for their advice.

References

[1] Application Software Group. CERN - CN Division,
GEANT - Detector Description and Simulation Tool

[2] A. Fassò et al., An Update About Fluka, Proceedings of the Second Workshop on Simulating Accelerator Radiation Environments, CERN, 9-11 October 1995, CERN/TIS-RP/97-05 and references therein

[3] J.B. Jeanneret et al., Quench Levels and transient Beam Losses in LHC Magnets, LHC Project Report 44, CERN, 1996

[4] K. Potter et al., Estimates of Dose to Components in the Arcs of the LHC due to Beam-Loss and Beam-Gas Interactions, LHC Project Note 18, CERN, 1995

[5] The LHC Study Group, P. Lefèvre, T. Pettersson (editors), The Large Hadron Collider - Conceptual Design, CERN/AC/95-05(LHC)

[6] J. Bosser et al., Preliminary Measurements on Micro-Calorimeters foreseen to be used as Beam-Loss Monitors, LHC Project Note 71, CERN, 1996

[7] B. Angerth et al., The Large Hadron Collider Vacuum System, Particle Accelerator Conference, Dallas, May 1995

[8] Y. Baconnier, J.B. Jeanneret and A. Poncet, LHC Beam Aperture and Beam Screen Geometry, MT Division Internal Note, MT/95-11 (ESH), LHC Note 326, CERN, June 1995

[9] J.B. Jeanneret, R. Ostojic, Geometrical Acceptance in LHC Version 5.0, LHC Project Note 111, CERN, 1997

[10] C. Bovet, J.B. Jeanneret, Tertiary Beam Losses in the LHC Arcs LHC Project Note 125, CERN, 1997

[11] H.C. Fesefeldt, Simulation of hadronic showers, physics and applications, Technical Report PITHA 85-02, III. Physikalisches Institut, RWTH Aachen Physikzentrum, Aachen, Germany, September 1985

[12] Magnetic fields were calculated with ROXIE 4.3 by S. Russenschuck, CERN - LHC Division

[13] W. Bialowons, F. Ridoutt and K. Wittenburg, Electron Beam Loss Monitors for HERA, Proceedings of the 4^{th} European Particle Accelerator Conference, London, 27 June - 1 July 1994

[14] F. Ridoutt, PIN-Strahlverlustmonitore und ihre Anwendung in dem HERA-Elektronenring, diploma thesis, University of Hamburg, DESY-HERA-95-08, October 1995

[15] The Tevatron beam position and beam loss monitoring systems, International Conference on High Energy Accelerators,
Fermilab 1983

[16] J. Bosser, CERN, private communication